ORIGINAL ARTICLE

Post-buckling reliability analysis of stiffened composite panels based on adaptive iterative sampling

Feng Zhang[1,2] · **Mingying Wu**[1] · **Xinting Hou**[1] · **Cheng Han**[1] · **Xinhe Wang**[1] · **Xiayu Xu**[1,3]

Abstract

The use of an adaptive iterative sampling method is proposed to analyze the post-buckling reliability of stiffened composite panel structures. First, a post-buckling yield strength model for a stiffened composite panel is established based on a semi-empirical equation, and its accuracy is experimentally verified. On this basis, a reliability analysis model is proposed for a stiffened composite panel. The probability of post-buckling failure is then estimated by the adaptive iterative sampling method. By continuously optimizing the sampling center and establishing an appropriate sampling function, the sampling efficiency of the reliability analysis is shown to be improved compared with the Monte Carlo method while ensuring a small relative error. The two-norm value of the sampling center position is shown to decrease continuously and converge to stability, meeting the accuracy requirements and providing a more reliable result. The proposed method, therefore, represents an efficient reliability evaluation method for stiffened composite panels that can be used to improve research into their post-buckling behavior.

✉ Feng Zhang
  nwpuwindy@nwpu.edu.cn

  Mingying Wu
  wumingying@mail.nwpu.edu.cn

  Xinting Hou
  hxtxinting@mail.nwpu.edu.cn

  Cheng Han
  hancheng@mail.nwpu.edu.cn

  Xinhe Wang
  wangxinhe0213@mail.nwpu.edu.cn

  Xiayu Xu
  XuXiayu@mail.nwpu.edu.cn

1   School of Mechanics, Civil Engineering and Architecture, Northwestern Polytechnical University, Xi'an 710129, China

2   Key Laboratory of Icing and Anti/De-Icing, China Aerodynamics Research and Development Center, Mianyang 621000, Sichuan, China

3   The Aviation Industry Corporation of China, Xi'an Flight Automatic Control Institute, Xi'an 710065, China

1 Introduction

Composite materials have the advantages of high specific strength, lightweight, and good chemical corrosion resistance, making them well-suited to widespread use in the aircraft industry [1, 2]. During aircraft use, stiffened composite structures are subjected to tensile, compressive, bending, shear, and impact loads that result in complex stress forms, with buckling being a common failure mode [3, 4]. When subjected to axial load, a stiffened composite panel will remain undamaged after buckling and still exhibit sufficient bearing capacity; that is, it has excellent post-buckling strength. The bearing efficiency of a structure can therefore be considerably improved by making full use of this characteristic [5, 6]. The study of the post-buckling reliability of stiffened composite structures thus has important value in engineering applications [7–12]. For example, Mohammed et al. [7] proposed a finite element modeling strategy to capture failure modes associated with steel bar buckling and low cycle fatigue. Salami et al. [8] proposed a nonlinear fiber beam-column model, which can simulate a variety of failure modes of reinforced concrete columns under dynamic loads. Huang et al. [9] combined with the random damage

constitutive model of concrete, and carried out numerical simulation work on material failure, member fracture and structural buckling.

Many scholars have studied the buckling of stiffened composite panels [13–18]. For example, Yu et al. [15] studied the post-buckling behavior of fixed laminated beams under axial compression and shear deformation, and established the analytical solution of the original governing equation. Guo et al. [16] studied the buckling and post-buckling of copper nanobeams under uniaxial compression by theoretical analysis and atomic simulation. Hu et al. [17] studied the axial and eccentric compression behavior of Q420 double angle composite columns. Sun et al. [18] established a seismic vulnerability analysis framework based on machine learning to assess the risk of structures under seismic loading.

In a traditional composite structure design, the mechanical model is first determined [19, 20], then the safety factor method is applied. This design method is able to reduce the instance of structural failure to some extent, but cannot completely prevent it. Indeed, due to the current lack of quantitative analyses on the variability of the relevant design parameters, any applied safety factor cannot accurately reflect the degree of safety of an engineering structure [21, 22]. A particularly large number of uncertainties exist in composite structures, including those related to material properties, geometric parameters, applied loads, and boundary conditions, etc., none of which are typically consistent. These uncertainties will notably have a significant impact on the performance of stiffened composite panels [23, 24]. Therefore, it is necessary to study the reliability of such composite structures [25, 26].

At present, the most commonly used methods for the reliability analysis of composite structures include approximate analytical methods [27] and digital simulation methods [28, 29]. Approximate analytical methods include the first-order second-moment method [30], which requires minimal calculation but results in a large relative error, making it only suitable for the reliability problem of an explicit limit state equation. Among the digital simulation methods, the Monte Carlo method [31] uses the joint probability density function of random variables for sampling. This method is simple, but its sampling efficiency is low so that large-scale calculation is necessary to obtain results that meet most accuracy requirements. The importance sampling method [32] is another type of digital simulation method that takes the design point of the limit state equation as the sampling center, considerably improving the sampling efficiency. However, this design point must be obtained in advance. When determining the post-buckling reliability of a stiffened composite panel, it is difficult to directly obtain the design point of the limit state equation, restricting the direct use of the importance sampling method. Therefore, the use of an adaptive iterative sampling method that is able to

continuously optimize the sampling center and estimate the failure probability using pre-sampling is proposed in this paper. In this method, the sampling efficiency—that is, the ratio of the number of samples falling into the failure area to the total number of samples—is defined during the process of sampling to provide a basis for the quantitative evaluation of optimality.

To study the post-buckling characteristics of stiffened composite panels and ensure full utilization of the excellent properties of composite materials, the failure limit stress of stiffened composite panels was calculated using a semi-empirical equation and the results were compared with the corresponding experimental results. A failure analysis of the stiffened composite panel was then conducted using the adaptive iterative sampling method, and the results were discussed. The results of this study indicate that the proposed adaptive iterative sampling method provides higher sampling efficiency, smaller error, and greater accuracy than the conventional Monte Carlo method, demonstrating that it is a more efficient and reliable method for post-buckling reliability research.

Nomenclature			
D	Bending stiffness	P_{cr}	Euler load
ET	Tensile and compressive stiffness	P_e	Buckling load
GT	Shear stiffness coefficient	σ_{co}	Failure stress
EI	Buckling stiffness	$Load$	Failure load

## 2 Post-buckling failure model of a stiffened composite panel

2.1 Post-buckling analysis based on semi-empirical equations

A sketch of the stiffened composite panel structure studied in this paper, consisting of a skin plate laminate and stiffeners, is shown in Fig. 1. To define the bending stiffness of the skin plate and overall stiffened panel, in this section, the post-buckling limit load of a stiffened composite panel is first calculated using semi-empirical equations [33] and a buckling analysis is conducted.

(1) The stiffness coefficients of the skin plate laminate are calculated by

$$A_{ij} = \sum_{k=1}^{M} \left(\overline{Q}_{ij}\right)_k \left(Z_k - Z_{k-1}\right) \tag{1}$$

Fig. 1 Structural diagram of the stiffened composite panel **a** stiffener and **b** skin plate laminate

(a)   **(b)**
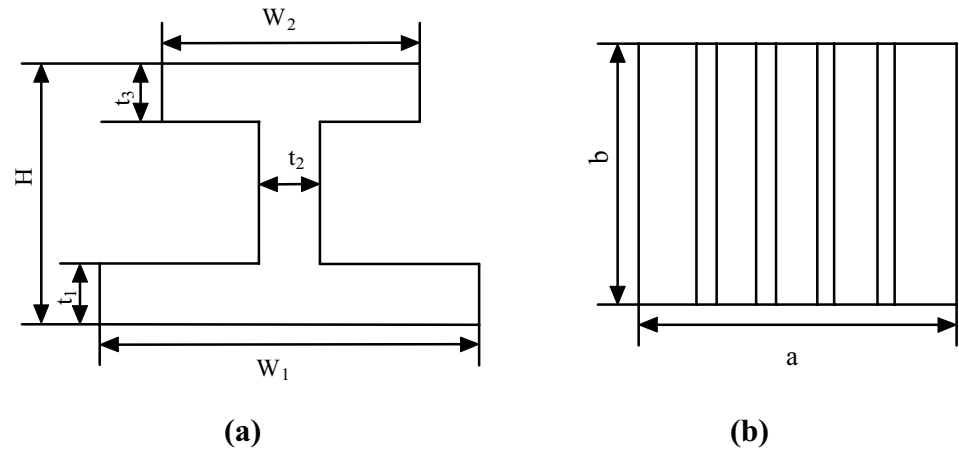
$$B_{ij} = \frac{1}{2} \sum_{k=1}^{M} \left(\overline{Q}_{ij}\right)_k \left(Z_k^2 - Z_{k-1}^2\right) \tag{2}$$

$$D_{ij} = \frac{1}{3} \sum_{k=1}^{M} \left(\overline{Q}_{ij}\right)_k \left(Z_k^3 - Z_{k-1}^3\right), \tag{3}$$

where A_{ij} is the in-plane stiffness coefficient of the laminate; B_{ij} is the tension bending stiffness coefficient of the laminate; D_{ij} is the bending stiffness coefficient of the laminate; i, j are the directions of stress, given as 1, 2, and 6; M is the total number of plies; Z_k and Z_{k-1} are the z-direction coordinates of plies k and k—1, respectively; and $(\overline{Q}_{ij})_k$ is the off-axis modulus of the k-th ply.

(2) The equivalent bending stiffness D of a symmetric laminate is calculated by

$$D_x = D_{11} + \frac{2D_{12}D_{16}D_{26} - D_{22}D_{16}^2 - D_{12}^2 D_{66}}{D_{22}D_{66} - D_{26}^2} \tag{4}$$

$$D_y = D_{22} + \frac{2D_{12}D_{16}D_{26} - D_{11}D_{26}^2 - D_{12}^2 D_{66}}{D_{11}D_{66} - D_{16}^2} \tag{5}$$

$$D_{xy} = \frac{2D_{12}D_{16}D_{26} - D_{11}D_{26}^2 - D_{22}^2 D_{16}}{D_{11}D_{12} - D_{12}^2}, \tag{6}$$

where D_x is the equivalent bending stiffness of the laminate along the x direction; D_y is the equivalent bending stiffness of the laminate along the y direction; D_{xy} is the equivalent in-plane bending stiffness of the laminate; and $D_{11}, D_{12}, D_{22}, D_{66}, D_{16}, D_{26}$ are the bending stiffness coefficients of the laminate for each direction of stress.

(3) The equivalent in-plane tensile/compressive stiffness coefficients along with the x and y directions, $(ET)_x$ and

$(ET)_y$, respectively, and shear stiffness coefficient GT of the laminate are calculated by

$$(ET)_x = E_x t = A_{11} + \frac{2A_{12}A_{16}A_{26} - A_{22}A_{16}^2 - A_{12}^2 A_{66}}{A_{22}A_{66} - A_{26}^2} \tag{7}$$

$$(ET)_y = E_y t = A_{22} + \frac{2A_{12}A_{16}A_{26} - A_{11}A_{26}^2 - A_{12}^2 A_{66}}{A_{11}A_{66} - A_{16}^2} \tag{8}$$

$$(GT) = G_{xy} t = A_{66} + \frac{2A_{12}A_{16}A_{26} - A_{22}A_{16}^2 - A_{11}A_{26}^2}{A_{11}A_{22} - A_{12}^2}, \tag{9}$$

where t is the thickness of the laminate; $A_{11}, A_{12}, A_{22}, A_{16}, A_{26}$, and A_{66} are the in-plane stiffness coefficients of the laminate; E_x and E_y are the equivalent tensile/compressive elastic moduli of the laminate in the x and y directions, respectively; and G_{xy} is the equivalent in-plane shear modulus of the laminate.

(4) The overall buckling stiffness EI of the stiffened panel is calculated by

$$EI = \sum_{i=1}^{n} \left[\left(D_{11i} - \frac{D_{12i}^2}{D_{22i}}\right) b_i + \left(A_{11i} - \frac{A_{12i}^2}{A_{22i}}\right) b_i \left(z_i - z_c\right)^2 \right], \tag{10}$$

where b_i is the width of the i-th strip element; z_c is the position of the neutral axis of the section of the stiffened laminate; and $(z_i - z_c)$ is the distance from the center of the section of the i-th element to the neutral axis.

(5) The overall bearing capacity of the stiffened panel is calculated by

$$P_{cr} = \frac{P_e}{1 + \lambda P_e / \left(G\overline{A} \right)} \tag{11}$$

$$P_e = \frac{c\pi^2(\text{EI})}{L^2}, \tag{12}$$

where the support coefficient c is 2.04; the shape factor λ is 1.2; P_{cr} is the Euler load; G is the equivalent shear stiffness of the vertical web; $\overline{A}$ is the area of the vertical web; and P_e is the buckling load.

(6) The failure stress σ_{co} of the stiffened laminate plate is calculated by

$$\sigma_{co} = \left[1 - \left(1 - \frac{\sigma_{cr}}{\sigma_{cc}} \right) \frac{\sigma_{cr}}{\sigma_r} \right] \sigma_{cc}, \tag{13}$$

where σ_r is the global buckling stress of the stiffened laminate calculated by the Euler equation without considering the effect of stiffness reduction after local buckling of either the skin plate or stiffener; σ_{cc} is the short-plate compressive failure stress of the stiffened laminate, which is approximately 0.75 times that of the pure compressive failure stress of the skin laminate; σ_{co} is the failure stress of the stiffened laminate; and σ_{cr} is the local buckling stress of the skin laminate.

(7) The failure load of the stiffened composite panel is obtained by

$$\text{Load} = \sigma_{co}A, \tag{14}$$

where σ_{co} is the failure stress of the stiffened laminate and A is it's area.

This study employed a composite skin plate thickness of 0.125 mm, ply angle of 0°, skin width a of 710 mm, horizontal edge strip width W_1 of 55 mm, horizontal edge strip width W_2 of 25 mm, edge strip height H of 45 mm, and the stiffened laminated plate length b of 570 mm, resulting in a post-buckling stiffened composite panel failure load of 1300 kN, as calculated by Eqs. (1)–(14).

2.2 Experimental verification of failure modes

Axial compression tests of stiffened composite panels with the same parameters as those used to calculate the failure load in Sect. 2.1 were then conducted as discussed in this section as shown in Fig. 2. The local buckling of the skin was observed to occur first, followed by the overall buckling failure of the stiffened plate. The test results are shown in the load–displacement curve in Fig. 3, which indicates that the maximum failure load was 1417.89 kN. The calculated failure load is compared with the experimental result in Table 1.

2.3 Post-buckling simulation of composite stiffened panels

Abaqus software is used to simulate the composite stiffened panel with the same parameters for simulation, and the load–displacement curve is obtained, as shown in Fig. 4 below.
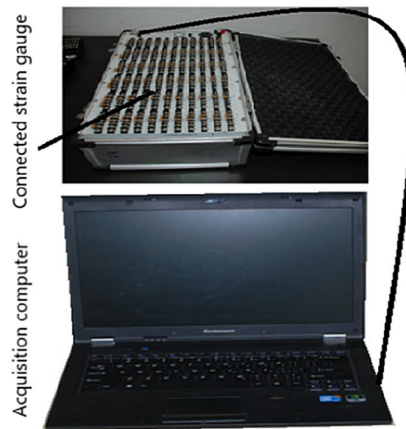
It can be seen from Fig. 4 that the simulation specimen is damaged at 1589 kN.

The calculated and simulated failure loads are compared with the experimental results in Table 1.

It can be observed in Table 1 that the experimentally obtained value agrees well with the value calculated using the semi-empirical equations, with a relative error

(a) Hydraulic testing machine   **(b)** Static strain gauge   **(c)** Failure of test piece

Fig. 2 Axial compression test

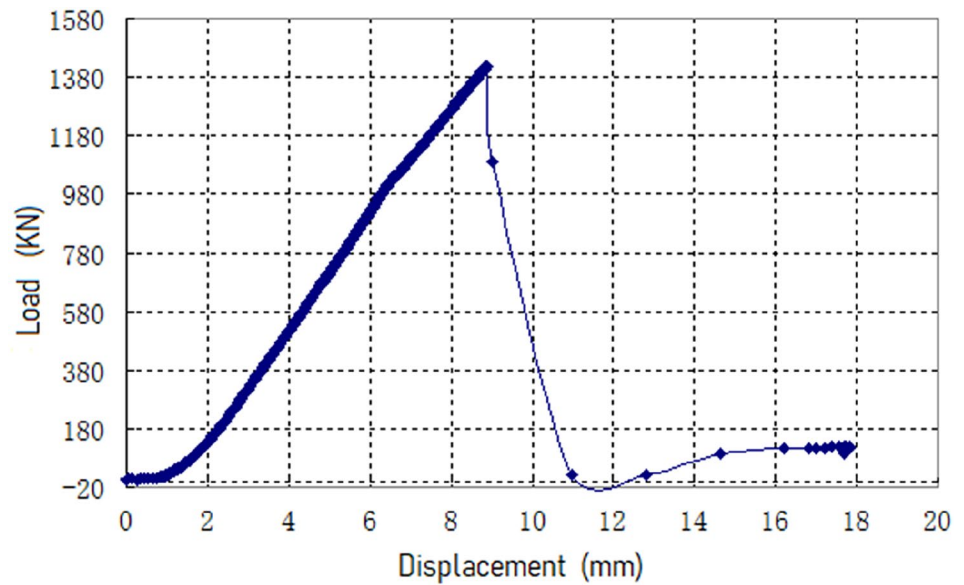**Fig. 3** Experimentally obtained load–displacement curve for the stiffened composite panel

Table 1 Comparison of results

Method	Failure load (kN)	Relative error
Experiment	1418	–
Simulation	1589	12.06%
Calculation	1300	8.3%

of approximately 8.3%. And when using Abaqus software, different people will get different results due to different mesh generation, while there is only one result calculated by semi-empirical equations. This indicates that the semi-empirical equations are highly accurate, establishing a good foundation for the subsequent structural reliability analysis.

3 Reliability analysis of stiffened composite panel post-buckling failure

3.1 Reliability modeling of post-buckling failure

There is a wide range of uncertainties in the structure of a stiffened composite panel, including the distribution of material properties, manufacturing process errors, and structural size deviations. Combining engineering experience and theoretical analysis, the thickness, width, and ply angle of the composite skin plate, as well as the edge strip widths, height, and length of the stiffened composite plate can be regarded as random variables, as defined in Table 2.

The failure load Load$\{X_1, X_2, \ldots, X_7\}$ can be obtained by substituting the relevant composite structure parameters into Eqs. (1)–(14). Combined with the actual load on the subject structure, the post-buckling analysis function is established as:

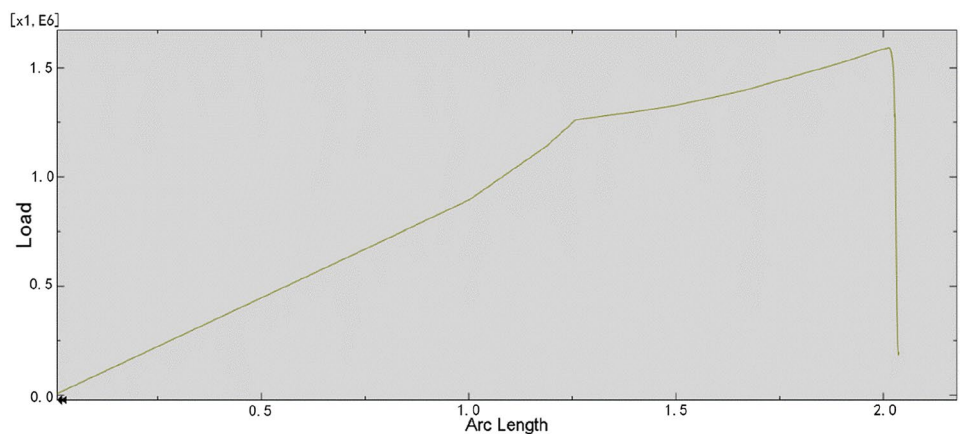**Fig. 4** Overall displacement-load diagram in Abaqus

Table 2 Probability characteristics of stiffened composite plate parameters

Parameter	Identification	Mean value	Standard deviation	Distribution type
Thickness (mm)	X_1	0.125	0.00125	Normal
Ply angle (°)	X_2	0	0.1	Normal
Skin width a (mm)	X_3	710	0.071	Normal
Horizontal edge strip width w_1 (mm)	X_4	55	0.0055	Normal
Horizontal edge strip width w_2 (mm)	X_5	25	0.0025	Normal
Edge strip height H (mm)	X_6	45	0.0045	Normal
Stiffened laminate length b (mm)	X_7	570	0.057	Normal
Actual load (N)	X_8	1.256×10^6	1×10^4	Normal

$$g(\mathbf{X}) = \text{Load}\{X_1, X_2, \dots, X_7\} - X_8, \tag{15}$$

where $\mathbf{X} = \{X_1, X_2, \dots, X_8\}$.

When $g(\mathbf{X}) < 0$ the post-buckling behavior X falls into the failure domain Rn; when $g(\mathbf{X}) \geq 0$, there is no failure, and X falls into the safety region Rs.

3.2 Adaptive iterative sampling method

The adaptive iterative sampling applied in this study is based on the Monte Carlo method. By constantly modifying the sampling center during the calculation process to limit it as much as possible to the "important areas" that have a significant impact on the results, the sampling of irrelevant events is minimized, improving the calculation efficiency.

The traditional method used for sampling in a structural reliability analysis is the Monte Carlo method. The integral equation expressing the Monte Carlo method used to determine failure probability is

$$P_{\mathrm{f}} = \int_{Rn} f(\mathbf{X})\mathrm{d}\mathbf{X}, \tag{16}$$

where $f(\mathbf{X})$ is the joint probability density function, which in this study is based on the variables $\mathbf{X} = \{X_1, X_2, \cdots, X_8\}^{\mathrm{T}}$; Rn is the failure domain; and P_{f} is the failure probability, which in this study is the evaluation index of the post-buckling reliability of the stiffened composite panel.

According to the joint probability density function $f(\mathbf{X})$, N samples $\{\mathbf{X}_1, \mathbf{X}_2, \cdots, \mathbf{X}_N\}^{\mathrm{T}}$ of input vector variable X are extracted, then the estimated value of failure probability $\hat{P}_{\mathrm{f}}$ is given by

$$\hat{P}_{\mathrm{f}} = \frac{1}{N}\sum_{s=1}^{N} I(\mathbf{X}_s) = \frac{N_{\mathrm{f}}}{N}, \tag{17}$$

where $\mathbf{X}_s$ is the s-th sample ($s = 1, 2, \dots, N$) extracted by the joint probability density function $f(\mathbf{X})$; $I(\mathbf{X})$ is the indicator function; $I(\mathbf{X}_s) = \begin{cases} 1 & \mathbf{X}_s \in Rn \\ 0 & \mathbf{X}_s \notin Rn \end{cases}$; N_{f} is the number of samples falling within the failure domain Rn, and N is the total number of samples.

The Monte Carlo method requires a large number of samples to obtain converging results, and its sampling efficiency is very low. Therefore, researchers have proposed improved digital simulation methods [29], of which the importance sampling method is one of the more common. By introducing the importance sampling density function $h(\mathbf{X})$, the integral equation for solving the failure probability is transformed into

$$P_f = \int_{Rn} \frac{f(\mathbf{X})}{h(\mathbf{X})} h(\mathbf{X})\mathrm{d}\mathbf{X} . \tag{18}$$

If N samples of input variable X are extracted according to the importance sampling density function $h(\mathbf{X})$, the estimated failure probability $\hat{P}_f$ is:

$$\hat{P}_{\mathrm{f}} = \frac{1}{N}\sum_{s=1}^{N}\left[I(\mathbf{X}_s)\frac{f(\mathbf{X}_s)}{h(\mathbf{X}_s)}\right]. \tag{19}$$

The challenge when using the importance sampling method to solve the reliability problem of the post-buckling behavior of stiffened composite panels is to select an appropriate importance sampling function $h(\mathbf{X})$. The simple explicit function $g(\mathbf{X})$ can be obtained by improving the first-order second-moment method. For the post-buckling problem of stiffened composite panels, the form of function $g(\mathbf{X})$ is complex, and it is difficult to obtain it directly. Therefore, in this study, the adaptive iterative strategy was used to modify the sampling center and construct the next sampling function.

For the adaptive iterative importance sampling function $h_q(\mathbf{X})(q = 1, 2, \dots, m)$, the number of samples extracted is $N_{(q)}(q = 1, 2, \dots, m)$. Therefore,

$$P_{f(q)} = \int_{Rn} \frac{f(\mathbf{X})}{h_{(q)}(\mathbf{X})} h_{(q)}(\mathbf{X})\mathrm{d}\mathbf{X} \tag{20}$$

$$\hat{P}_{f(q)} = \frac{1}{N_{(q)}}\sum_{s=1}^{N_{(q)}}\left[I_F(\mathbf{X}_{(q)s})\frac{f(\mathbf{X}_{(q)s})}{h_{(q)}(\mathbf{X}_{(q)s})}\right]. \tag{21}$$

Finally, the failure probability estimation based on the adaptive iterative importance sampling method can be defined as

$$\hat{P}_f = \frac{1}{m} \sum_{q=1}^{m} \hat{P}_{f(q)} \tag{22}$$

To effectively evaluate the sampling efficiency of the proposed method, the sampling efficiency η is defined as the ratio of the number of samples falling into the failure area Rn to the total number of samples.

The sampling efficiency η of the Monte Carlo method is given by

$$\eta = \frac{N_f}{N} = P_f. \tag{23}$$

For the adaptive iterative importance sampling method, if the number of samples falling into the failure area in the q-th $(q = 1, 2, \ldots, m)$ sampling is $N_{(q)f}(q = 1, 2, \ldots, m)$, then the sampling efficiency η_q is

$$\eta_q = \frac{N_{(q)f}}{N_{(q)}}. \tag{24}$$

Thus, the total sampling efficiency η for the adaptive iterative sampling is

$$\eta = \frac{\sum_{q=1}^{m} N_{(q)f}}{\sum_{q=1}^{m} N_{(q)}}. \tag{25}$$

3.3 Obtaining failure probability

According to the principle of the adaptive iterative importance sampling method, the specific steps used to calculate the post-buckling reliability of a stiffened composite panel are as follows.

1. The first importance sampling function is $h_{(1)}(\mathbf{X})$, and the sampling center $\mathbf{\Delta}_{\mathbf{X}(1)}$ of $h_{(1)}(\mathbf{X})$ is its mean point. The variance vector of the sampling function is consistent with the variance vector of the joint probability density function of the input vector, that is, $\mathbf{\mu}_{h(1)} = \mathbf{\mu}_{\mathbf{X}}$ and the variance vector $\mathbf{\sigma}_{h(1)}^2 = \mathbf{\sigma}^2$. According to the importance sampling function $h_{(1)}(\mathbf{X})$, $N_{(1)}$ samples are selected to judge whether the sample $\mathbf{X}_{(1)s}(s = 1, 2, \ldots, N_{(1)})$ falls into the failure region Rn. For the sampling points falling into Rn, the failure probability is calculated by Eq. (21), and the sample point corresponding to the current maximum value of $f(\mathbf{X})$ is marked as $\mathbf{\delta}*$. The sampling center $\mathbf{\Delta}_{\mathbf{X}(2)}$ of the second importance sampling function $h_{(2)}(\mathbf{X})$ is thus defined as

$\mathbf{\delta}^*$. The variance vector of the second importance sampling function is consistent with the variance vector of the joint probability density function of the input vector.

2. The q-th $(q = 2, 3, \ldots, m)$ importance sampling density function $h_{(q)}(\mathbf{X})$ is normal, and the sampling center is $\mathbf{\Delta}_{\mathbf{X}(q)}$. The variance vector of this importance sampling density function is consistent with the variance vector of the joint probability density function of the input vector; that is, $\mathbf{\mu}_{h(q)} = \mathbf{\Delta}_{\mathbf{x}(q)}$ and the variance vector $\mathbf{\sigma}_{h(q)}^2 = \mathbf{\sigma}^2$. According to the importance sampling function $h_{(q)}(\mathbf{X})$, $N_{(q)}$ samples are selected to judge whether sample $\mathbf{X}_{(q)s}(s = 1, 2, \ldots, N_{(q)})$ falls into the failure region Rn. For the sampling points falling into Rn, the failure probability is calculated by Eq. (21), and the sample point corresponding to the current maximum value of $f(\mathbf{X})$ is marked as $\mathbf{\delta}*$. Then, the joint probability density functions $f(\mathbf{\Delta}_{\mathbf{X}(q)})$ and $f(\mathbf{\delta}*)$, respectively corresponding to $\mathbf{\Delta}_{\mathbf{X}(q)}$ and $\mathbf{\delta}*$ are compared; if $f(\mathbf{\delta}*) \geq f(\mathbf{\Delta}_{\mathbf{X}(q)})$, the sampling center $\mathbf{\Delta}_{\mathbf{X}(q+1)}$ of the $(q+1)$-th importance sampling function $h_{(q+1)}(\mathbf{X})$ is selected as $\mathbf{\delta}*$; otherwise, the sampling center $\mathbf{\Delta}_{\mathbf{X}(q+1)}$ of the $(q+1)$-th importance sampling function $h_{(q+1)}(\mathbf{X})$ is selected as $\mathbf{\Delta}_{\mathbf{X}(q)}$.

3. A total of M samplings are conducted. The failure probability $\hat{P}_f$ of the stiffened composite panel structure is calculated by Eq. (22), and the algorithm is finished.

The flow chart for determining the failure probability using the proposed adaptive iterative sampling method is shown in Fig. 5.

4 Analysis and discussion

The typical method for reliability modeling and analysis primarily relies upon the collection of a large quantity of failure data to design and evaluate the reliability based on probability theory. In this study, a reliability analysis is applied to quantitatively determine the post-buckling reliability of stiffened composite panels based on probability and statistics.

In this study, the adaptive iterative sampling method was used for the reliability analysis. In order to evaluate the calculation accuracy and efficiency of this method, its results are compared with those of the Monte Carlo method in Table 3.

It can be seen from the results in Table 3 that for the same total number of samples, the relative error between the results obtained using the adaptive iterative sampling method and those obtained using the Monte Carlo method is only $=\delta$ $(5.6077\times10^{-5}–5.525\times10^{-5})/(5.6077\times10^{-5}) = 1.47\%$, which indicates consistent results. It can be seen in Fig. 6 that the
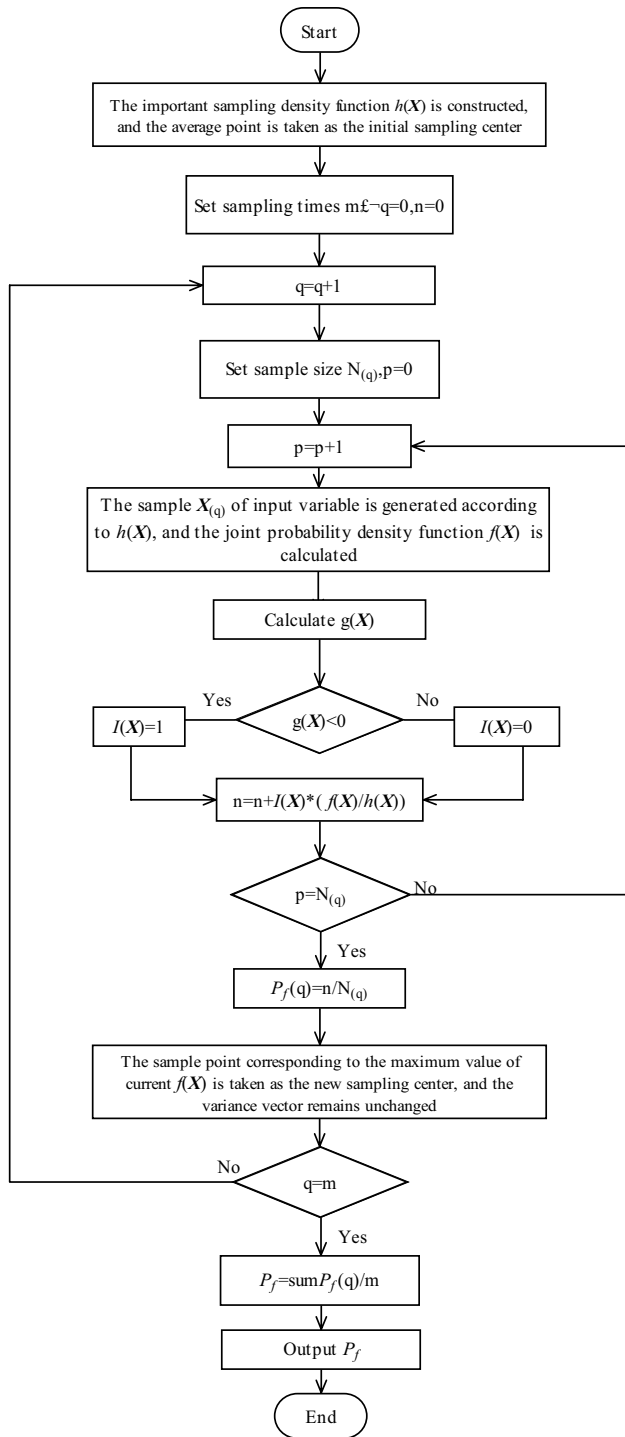
Fig. 5 Flow chart for determining failure probability using the adaptive iterative sampling method

failure probability curve corresponding to the adaptive iterative sampling method fluctuates only slightly, while that corresponding to the Monte Carlo method fluctuates relatively large. This demonstrates that compared with the traditional Monte Carlo method, the failure probability obtained by the adaptive iterative sampling method tends to stability much faster. Indeed, the simulation times required to obtain a convergent solution using the proposed method are much less than those using the Monte Carlo method, indicating improved efficiency. Comparing the total sampling efficiency of the adaptive iterative sampling method with that of the Monte Carlo method as reported in Table 3, an improvement of $0.4912/(5.4 \times 10^{-5}) = 8.8931 \times 10^3$ can be observed. Therefore, the adaptive iterative sampling method is just as accurate as the Monte Carlo method, but much more efficient.

The two-norm describes the linear distance between two vector matrices in space. By calculating the two-norm of the sampling center positions obtained in each iteration of the adaptive iterative sampling process, we can observe the correction of sampling centers between iterations.

In normal space, the two-norm of the sampling center position in the adaptive iterative sampling method can be calculated by.

$$\frac{\Delta_X - \mu_X}{\sigma} \tag{26}$$

with the results shown per iteration in Table 4 and Fig. 7.

It can be seen in Table 4 that the two-norm of the sampling center consistently decreases with increasing iterations. Starting at the fourth sampling iteration, the two-norm of the sampling center changes only slightly in the next iteration, indicating that the sampling center is constantly being adaptively adjusted.

It can be seen in Table 4 that after many iterations, the two-norm of the sampling center position in the normal distribution decreases and gradually converges to a stable value. From the plot of two-norm sampling center position in Fig. 7, it can be confirmed that the overall curve shows a decreasing trend with a very small fluctuation, proving that there is an optimal design point. The selection of design point directly affects the efficiency and accuracy of the calculation as the adaptive iterative sampling method depends on the selection of design points. The existence of an optimal design point thus indicates that the results obtained using the adaptive iterative sampling method are reliable, stable, and

Table 3 Resulting failure probability according to the calculation method

	Failure probability p_f	Samples	Sampling efficiency
Monte Carlo method	5.525×10^{-5}	4×10^6	5.4×10^{-5}
Adaptive iterative sampling method	5.6077×10^{-5}	4×10^6	0.4913

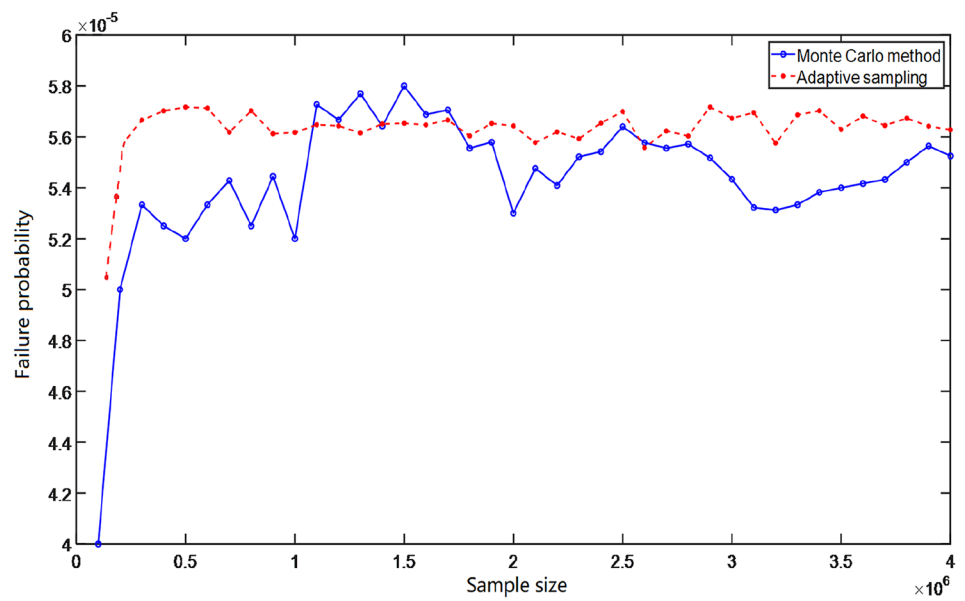**Fig. 6** Change in probability of failure with sample size

Table 4 Two-norms of sampling center location

Number of iterations	Total samples	Two-norm of sampling center	Sampling efficiency
1	200,000	4.5842	5×10^{-5}
2	400,000	3.9435	0.6577
3	600,000	3.9213	0.5083
4	800,000	3.9156	0.5068
5	1,000,000	3.9156	0.5108
6	1,200,000	3.9156	0.5119
7	1,400,000	3.9156	0.5112
8	1,600,000	3.9156	0.5111
9	1,800,000	3.9156	0.5100
10	2,000,000	3.9156	0.5099
11	2,200,000	3.9156	0.5115
12	2,400,000	3.9156	0.5093
13	2,600,000	3.9156	0.5101
14	2,800,000	3.9156	0.5116
15	3,000,000	3.9156	0.5128
16	3,200,000	3.9150	0.5112
17	3,400,000	3.9150	0.5085
18	3,600,000	3.9102	0.5086
19	3,800,000	3.9102	0.5028
20	4,000,000	3.9102	0.5028

effective. It is therefore proven that the proposed use of the adaptive iterative sampling method can effectively analyze the post-buckling reliability of stiffened composite panels.

5 Conclusion

In this study, a semi-empirical equation was first derived and used to determine the ultimate load of a stiffened composite panel, which was then experimentally verified; the experimental and semi-empirical results agreed well, and the error is about 8.3%. It was then demonstrated that some processing methods and algorithms for capturing uncertainty in the semi-empirical equations are more effective and accurate than others. Based on the semi-empirical equations, the post-buckling reliability of a stiffened composite panel was then analyzed and discussed using the proposed adaptive iterative sampling method to obtain the failure probability. Compared with the traditional Monte Carlo method, the adaptive iterative sampling method was shown to reduce the sampling of events that are irrelevant to the analysis results, improving the calculation efficiency. Notably, the adaptive iterative sampling method is independent as it did not need to find the sampling center of the panel using any other method. An analysis and discussion of the two-norm of the sampling center position during sampling indicated that after several iterations, its value gradually decreases and converges to stability. This proved that there was an optimal design point, indicating that the adaptive iterative sampling method based on the derived semi-empirical equations is effective and the results obtained are reliable and stable. The results of this research are of significance to the study of the post-buckling reliability of stiffened composite panels and can be used to improve and consolidate the application of composite materials in aircraft.

Fig. 7 Change in two-norm of sampling center position according to sample size
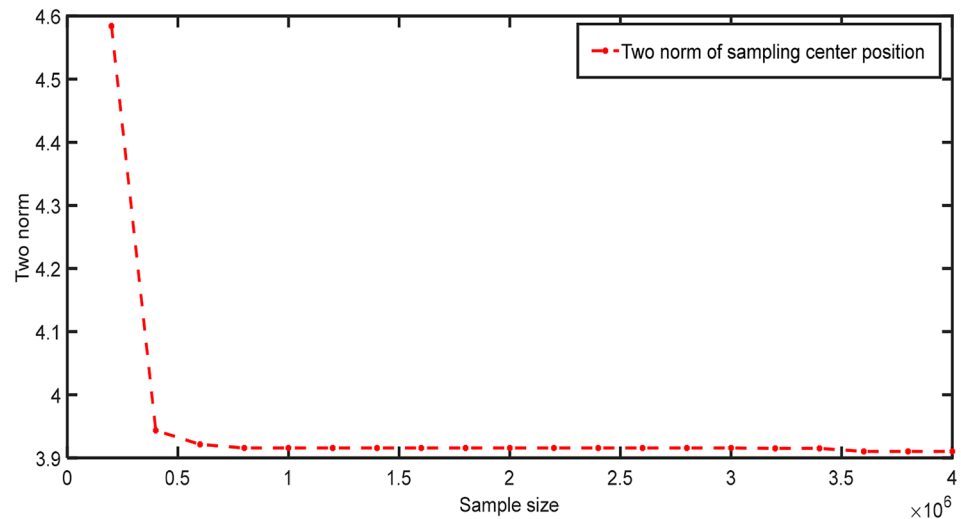
References

1. Karthigeyan P, Senthil Raja M, Hariharan R, Karthikeyan R, Prakashc S (2017) Performance evaluation of composite material for aircraft industries. Mater Today Proc 4:3263–3269

2. Turczyn R, Krukiewicz K, Katunin A et al (2020) Fabrication and application of electrically conducting composites for electromagnetic interference shielding of remotely piloted aircraft systems. Compos Struct 232:111498

3. Zimmermann N, Wang PH (2020) A review of failure modes and fracture analysis of aircraft composite materials. Eng Fail Anal 115:104692

4. Luo Y, Zhan J, Liu P (2019) Buckling assessment of thin-walled plates with uncertain geometrical imperfections based on non-probabilistic field model. Thin-Walled Struct 145:106435

5. Vummadisetti S, Singh SB (2020) Buckling and postbuckling response of hybrid composite plates under uniaxial compressive loading. J Build Eng 27:101002

6. Zhao L, Wang K, Ding F et al (2019) A post-buckling compressive failure analysis framework for composite stiffened panels considering intra-, inter-laminar damage and stiffener debonding. Results Phys 13:102205

7. Mohammed MA, Barbosa AR (2019) Numerical modeling strategy for the simulation of nonlinear response of slender reinforced concrete structural walls. CMES Comput Model Eng Sci 120:583–627

8. Salami MR, Dizaj EA, Kashani MM (2019) the behavior of rectangular and circular reinforced concrete columns under biaxial multiple excitation. Comput Model Eng Sci 120:677–691

9. Huang T, Zhou H, Beiraghi H (2020) Collapse Simulation and response assessment of a large cooling tower subjected to strong earthquake ground motions. CMES Comput Model Eng Sci 123(2):691–715

10. Han J, Wan C, Fang H, Bai Y (2020) Development of self-floating fibre reinforced polymer composite structures for photovoltaic energy harvesting. Compos Struct 253:112788

11. Guo S, Li W (2020) Numerical analysis and experiment of sandwich T-joint structure reinforced by composite fasteners. Compos B 199:108288

12. Chen X, Qiu Z (2018) Reliability assessment of fiber-reinforced composite laminates with correlated elastic mechanical parameters. Compos Struct 203:396–403

13. Luo Y, Bao J (2019) A material-field series-expansion method for topology optimization of continuum structures. Comput Struct 225:106122

14. Luo Y, Zhan J (2020) Linear buckling topology optimization of reinforced thin-walled structures considering uncertain geometrical imperfections. Struct Multidiscip Optim 62(4):3367–3382

15. Yu Y, Chen L, Zheng S, Zeng B, Sun W (2020) Closed solution for initial post-buckling behavior analysis of a composite beam with shear deformation effect. CMES Comput Model Eng Sci 123(1):185–200

16. Guo J, Yunfei Xu, Jiang Z, Liu X, Cai Y (2020) A simplified model for buckling and post-buckling analysis of Cu nanobeam under compression. CMES Comput Model Eng Sci 125(2):611–623

17. Hu H, He J, Song L, Zhan Z, Li Z (2019) experimental study and finite element analysis on ultimate strength of dual-angle cross combined section under compression. CMES Comput Model Eng Sci 119:499–539

18. Sun B, Zhang Y, Huang C (2020) Machine Learning-Based Seismic Fragility Analysis of Large-Scale Steel Buckling Restrained Brace Frames. CMES-Comput Model Eng Sci 125(2):755–776

19. Deleo AA, O'Neil J, Yasuda H et al (2020) Origami-based deployable structures made of carbon fiber reinforced polymer composites. Compos Sci Technol 19:108060

20. Bheemreddy V, Huo Z, Chandrashekhara K, Brack RA (2014) Process modeling of cavity molded composite flex beams. Finite Elem Anal Des 78:8–15

21. Wang X, Shi Q, Fan W et al (2019) Comparison of the reliability-based and safety factor methods for structural design. Appl Math Model 72:68–84

22. Kövesdi B, Somodi B (2018) Comparison of safety factor evaluation methods for flexural buckling of HSS welded box section columns. Structures 15:43–55

23. Sun R, Chen G, He H, Zhang B (2014) The impact force identification of composite stiffened panels under material uncertainty. Finite Elem Anal Des 81:38–47

24. Noor AK, Starnes JH Jr, Peters JM (2001) Uncertainty analysis of stiffened composite panels. Compos Struct 51:139–158
25. Zhang F, Xiayu Xu, Cheng L, Tan S, Wang W, Mingying Wu (2020) Mechanism reliability and sensitivity analysis method using truncated and correlated normal variables. Saf Sci 125:104615
26. Chen X, Wang X, Qiu Z et al (2018) A novel reliability-based two-level optimization method for composite laminated structures. Compos Struct 192:336–346
27. Hurtado JE, Alvarez DA (2013) A method for enhancing computational efficiency in Monte Carlo calculation of failure probabilities by exploiting FORM results. Comput Struct 117:95–104
28. Chen H, Mao Z-l (2018) Study on the failure probability of occupant evacuation with the method of monte carlo sampling. Proce Eng 211:55–62
29. Liu X, Elishakoff I (2020) A combined Importance Sampling and active learning Kriging reliability method for small failure probability with random and correlated interval variables. Struct Saf 82:101875
30. Yang Z, Ching J (2020) A novel reliability-based design method based on quantile-based first-order second-moment. Appl Math Model 88:461–473
31. Ling C, Zhenzhou Lu, Sun Bo, Wang M (2020) An efficient method combining active learning Kriging and Monte Carlo simulation for profust failure probability. Fuzzy Sets Syst 387:89–107
32. Nassim R, Marco CP (2018) Novel algorithm using active metamodel learning and importance sampling: application to multiple failure regions of low probability. J Comput Phys 368:92–114
33. China Academy of Aeronautics (2002) Guidelines for stability analysis of composite structures. Aviation Industry Press, Beijing